Trends in Analytical Chemistry 158 (2023) 116830

Contents lists available at ScienceDirect

Trends in Analytical Chemistry

journal homepage: www.elsevier.com/locate/trac

Molecularly imprinted polymer-based electrochemical sensors for food contaminants determination

Viknasvarri Ayerdurai [a], Maciej Cieplak [a, *], Wlodzimierz Kutner [a, b, **]

[a] Institute of Physical Chemistry, Polish Academy of Sciences, Kasprzaka 44/52, 01-224, Warsaw, Poland
[b] Faculty of Mathematics and Natural Sciences. School of Sciences, Cardinal Stefan Wyszynski University in Warsaw, Wóycickiego 1/3, 01-815, Warsaw, Poland

ARTICLE INFO

Article history:
Received 22 August 2022
Received in revised form
8 November 2022
Accepted 12 November 2022
Available online 17 November 2022

Keywords:
Molecularly imprinted polymer
Food toxin
Chemosensor
Electrochemical sensor
Food safety

ABSTRACT

The critical food safety assessment is one of the essences of the modern food industry. The major factors contributing to this assessment include the increased public awareness of safe food and the surge in quantity and variety of food pollutants because of globalization, industrialization, and population growth. With molecularly imprinted polymer (MIP) recognition units, electrochemical sensors have opted for food analysis in recent decades. MIP-based electrochemical sensors are versatile as they can be devised for different food contaminants. They offer simplicity in terms of sensor preparation and measurement and cost-efficiency. These sensors' affinity to target analytes is often high. In effect, the number of publications reporting MIP electrochemical chemosensors for food safety and quality monitoring applications has significantly increased. Therefore, the present review highlights the recent developments in fabricating MIP recognition-units-based electrochemical sensors and their applications in determining contaminants in various food and drink matrices.

1. Introduction

Bloom of the human population contributed to the significant increase in demand for food products and their variety. Although food production at the global scale has surpassed population growth since the 1960s, its safety is under scrutiny more now than ever [1]. Farmers and producers cultivate crops with extensive use of pesticides, insecticides, herbicides, artificial fertilizers, as well as veterinary and fishery drugs to increase crop production to meet the quantitative market demand. Different stages of food preparation, i.e., producing, processing, packaging, distributing, and retailing, expose food products to contaminants, including plasticizers, heavy metal ions, additives, preservatives, food dyes, and artificial fragrances. Moreover, some food and water may be contaminated with environmental pollutants, including allergens, natural toxins, and pathogens. Consumption of these chemical and biological hazardous substances and microorganisms has adverse effects, e.g., high blood pressure, allergic reactions, hypertension, hormonal dysfunction, inflammation, etc., on the consumers' health [2].

Food safety control is not easy despite active governmental efforts to control and monitor food quality. Analytical techniques, e.g., high-performance liquid chromatography (HPLC), combined with mass spectrometry (HPLC-MS), nuclear magnetic resonance (NMR) spectroscopy, etc., and methods, e.g., (polymerase chain reaction)-(gas chromatography) combined with mass spectrometry (MS) and enzyme-linked immunosorbent assay (ELISA), are currently opted to perform food quality and safety tests [3]. These techniques offer high accuracy. However, they require qualified operators, expensive instrumentation, and time-consuming, complicated measurements. Moreover, they are inadequate for determining various chemical contaminants in today's food products, often in trace amounts [2]. Therefore, a practical, cost-effective, and rapid detection with a high-throughput method that can be utilized at an industrial scale is in demand. Newly developed analytical methods should be easy to integrate with portable, hand-held devices, thus enabling on-spot sample analysis [4].

Electrochemical chemosensing combined with molecular imprinting in polymers can overtake conventional chemosensing methods as it fulfills all the food quality monitoring requirements.

* Corresponding author.
** Corresponding author. Institute of Physical Chemistry, Polish Academy of Sciences, Kasprzaka 44/52, 01-224, Warsaw, Poland.
E-mail addresses: mcieplak@ichf.edu.pl (M. Cieplak), wkutner@ichf.edu.pl (W. Kutner).

https://doi.org/10.1016/j.trac.2022.116830

Abbreviations

Acrylamide (AM)
Ammonium persulfate (APS)
2-Amino-3,7,8-trimethyl-3*H*-imidazo[4,5-f] quinoxaline (7,8-DiMeIQx)
Anodic stripping voltammetry (ASV)
Azobisisobutyronitrile (AIBN)
Bisphenol A (BPA)
Bisphenol AF (BPAF)
Carbon nanotubes (CNTs)
Cross-linking monomer (CRL)
Cyclic voltammetry (CV)
Dichlorodiphenyltrichloroethane (DDT)
Differential pulse voltammetry (DPV)
Dioctyl phthalate (DOP)
Enzyme-linked immunosorbent assay (ELISA)
Ethyl glycol dimethyl methacrylate (EGDMA)
Ethylene glycol methacrylate phosphate (EGMP)
Ferrocenecarboxylic acid (FcCOOH)
Flow-injection analysis (FIA)
Fumonisin B_1 (FB_1)
Functional monomer (FM)
Glassy carbon electrode (GCE)
Heat-transfer method (HTM)
High-performance liquid chromatography (HPLC)
High-performance liquid chromatography combined with mass spectrometry (HPLC-MS)
Imprinting factor (*IF*)
Lateral flow device (LFD)
Limit of detection (LOD)
Linear sweep voltammetry (LSV)
Methacrylic acid (MAA)
3-Methacryloxypropyltrimethyloxysilane (MPS)
Molecularly imprinted polymer (MIP)
Multi-walled carbon nanotubes (MWCNTs)
Nanoparticle (NP)
2-Nitrophenyl octyl ether (NPOE)
N-Hydroxysuccinimide (NHS)
N-Isopropylacrylamide (NIPAM)
N-Tertbutylacrylamide (TBAM)
Nuclear magnetic resonance (NMR)
Spectroscopy, ochratoxin A (OTA)
Ochratoxin D (OTD)
o-*N*,*N*′-Methylenebisacrylamide (BIS)
o-Phenylenediamine (*o*-PD)
Poly(ionic liquid) (pIL)
Poly(vinyl chloride) (PVC)
Polypyrrole (PPy)
Screen-printed carbon electrode (C-SPE)
Screen-printed electrode (SPE)
Signal-to-noise ratio (S/N)
Sodium salt of flavin mononucleotide (FMNS)
Sodium tetraphenylborate (NATPB)
Square-wave voltammetry (SWV)
Surface plasmon resonance (SPR)
Tetrahydrofuran (THF)
Tetramethylethylenediamine (TEMED)
Tridodecylmethylammonium chloride (TDMAC)
Vinyltrimethoxysilane (VTMOS)

Molecularly imprinted polymers (MIPs) are artificial molecular recognition polymeric materials that mimic biological recognition entities, such as antibodies, active centers of enzymes, aptamers, etc. They can be considered synthetic analogs to nature's enzyme-substrate systems, which operate based on Fischer's lock and key mechanism [5]. In this model, the receptor molecule and its natural target molecule are structurally complementary, allowing for their perfect fit. As a result, only the interacting molecules of the proper size, shape, and complementary functionality would fit into the active sides of the receptors. MIPs' ability to operate based on this unique interaction yields high affinity and selectivity. Moreover, in contrast to their biological counterparts, MIPs are chemically and mechanically stable under harsh chemical and physical conditions [6].

Due to their significant advantages, MIPs were primarily utilized in food analysis for analytical separation and purification using solid-phase extraction and chromatography [7]. In recent years, MIPs gained popularity as selective recognizing units of electrochemical chemosensors [8]. With small, portable equipment, MIP-based electrochemical sensors can detect analytes efficiently, sensitively, and inexpensively [2,9].

The present short review article highlights the most recent progress in MIP electrochemical chemosensors' fabrication and application in food quality and safety control (Scheme 1). The latest approaches, i.e., different electrochemical transduction methods used for MIP chemosensors performance improvement and perspective of future practical applications of MIP chemosensors in food quality and safety control, are discussed.

2. Molecularly imprinted polymers (MIPs)

The basic principle of molecular imprinting consists in imprinting in synthetic materials molecular cavities that complementarily fit the target analyte molecules. MIP's synthesis and operation involve four consecutive steps [10].

(i) The first involves forming stable pre-polymerization complexes of the target analyte, which at this step plays the role of a template, with selected functional monomers (FMs) in the solution. Depending on the chemical functionalities of these monomers, they can interact with the template/analyte molecules by forming covalent bonds or in a non-covalent way, i.e., via hydrogen bonds, electrostatic attractions, π-π stacking, hydrophobic and van der Waals interactions, etc.
(ii) The second step involves polymerizing the template-FM pre-polymerization complex in solution in the presence of the cross-linking monomers (CRLs). During this polymerization, the polymer net grows around these complexes' molecules. That way, the template is imprinted in the resulting rigid MIP matrix.
(iii) The third step is removing the template from the MIP, thus vacating molecular cavities that resemble the template/analyte molecules' shapes, sizes, and functionality distribution. That way, the emptied imprinted molecular cavities afford the MIP "memory" for the template/analyte.
(iv) The fourth step is the immersion of MIP in the analyte and interferences-containing test solution. The MIP molecular

cavities can recognize only the complementary analyte molecules, thus contributing to the MIP selectivity.

The morphology, properties, and performance of the MIPs are governed by the careful selection of FMs, CRLs, and porogenic solvents. MIPs are cautiously designed using different preparation and synthesis methods depending on the desired application [11]. Detailed, high-quality reviews on general MIP applications are reported elsewhere [12–15].

3. Electrochemical MIP chemosensors

Electrochemical sensors comprise two major parts, namely, a receptor and a transducer. In biosensors, numerous elements of biological origin, namely, enzymes, antibodies, aptames, receptors, DNA, phages and whole cells are applied [16–18]. However, MIPs deposited on the electrode surface serve as selective recognition units as well [13]. The electrochemical transducer converts the chemical recognition event into a quantifiable analytical signal, namely, current (A), charge (C), potential (V), resistance (Ω), or conductivity (S) [13,19]. For food safety assaying between 2010 and 2021, voltammetry was the most popular technique, followed by amperometry and impedimetry (see Table 1).

MIP electrochemical chemosensors propose two common strategies for determining target analytes (Scheme 1). The direct analytical measurement is performed for electroactive analytes [20–24] in the potential range of the analyte electroactivity, i.e., where direct electron transfer between the electroactive analyte and the transducer surface occurs. Voltammetry [20,21] and amperometry [24] are superior for quantifying electroactive targets. Charged analytes are often determined using potentiometry [25–27]. Moreover, the adsorption of electroinactive analytes on the electrode surface may be followed using changes in electrochemical double-layer capacity [28,29].

The indirect analytical signal is measured with an external redox probe, e.g., hexacyanoferrate, ferrocene, hexaammineruthenium(III) chloride, etc., added to the test solution to determine electro-inactive analytes [30–41]. The measurement is performed in the potential range, in which the redox probe is electroactive, and the faradaic current of this probe is the output signal. This indirect approach is known as the “gate effect” [39–41]. Importantly, electrochemical impedance spectroscopy (EIS) can be applied not only to study details of the electrode process mechanism but also to measure the charge transfer resistance change (ΔR_{ct}) originating from the “gate effect,” which may serve as the analytical signal [36].

3.1. Voltammetric MIP chemosensors

Voltammetric chemosensors are the most prevalent among electrochemical chemosensors as they offer fast and sensitive determination and simple preparation at a low cost. They measure the faradaic current of a redox reaction at an appropriate potential. The faradaic current measured linearly depends on the concentration of the analyte undergoing an electrochemical reaction [42]. There are a few modes of potential modulation, e.g., linear scanning with time, non-linear modulating with a pulse or sinusoidal excitation, etc. Depending on the type of potential agitation, voltammetric techniques fall into the category of cyclic voltammetry (CV) [20,30,31], linear sweep voltammetry (LSV) [22], differential pulse voltammetry (DPV) [32,33,37,38,43], square-wave voltammetry (SWV) [34,35,44], anodic stripping voltammetry (ASV) [23], etc. Particularly, the DPV technique has recently gained enormous attention as it offers a high signal-to-noise ratio and, hence, a sensitivity higher than other techniques [45].

3.1.1. Linear sweep voltammetry (LSV) MIP chemosensors

Wu et al. proposed a highly sensitive and stable sensor of (molecularly imprinted polypyrrole)-(multi-walled carbon nanotubes)-(glassy carbon electrode), (PPy)-MIP/MWCNTs/GCE, for amaranth determination (Scheme 2a) [22]. Innovatively, the template was eluted by overoxidizing the PPy film without losing the film's integrity. There were two linear concentration ranges, namely, from 7 nM to 1.0 μM and 0.4–17 μM, with the limit of detection (LOD) of 0.4 nm. The highly conductive PPy and MWCNTs contributed to the LSV amaranth signal amplification. Moreover, the large electroactive surface area of MWCNTs effectively accelerated the electron-transfer. The chemosensor determined amaranth in soft drinks, including watermelon, grape, and orange juices, with a 95.9–97.7% recovery.

3.1.2. Cyclic voltammetry (CV) MIP chemosensors

Wang et al. recently proposed a sensor of an MIP immobilized at silicon dioxide nanobeads coating MWCNTs deposited on gold nanoparticles layered on GCE, (MIP@SiO_2)/AuNPs/GCE, for dibutyl phthalate determination [30]. Dibutyl phthalate is a plasticizer that can easily leach and contaminate food and drinks as it is weakly bonded to the plastic through hydrogen and van der Waals bonding. This chemosensor determined dibutyl phthalate in real tap water samples and Chinese baijiu. The recovery exceeded 84%. The sensor was exceptionally sensitive, stable, and reproducible due to the multi-level electrode modification with MWCNTs and AuNPs, enhancing the electron transport rate. Moreover, the porous and open structure of the SiO_2 nanobeads decreased nonspecific adsorption by significantly increasing MIPs' surface area.

Interesting Au electrode modification with a nanowell Au film was proposed to determine 17β-estradiol, a sex steroid hormone [31]. The unique sponge-like 3D structure of the nanowell was why the surface area and several uniformly distributed molecular recognizing sites were high, making their availability for analyte binding high (Scheme 2b). Moreover, it enhanced the electron transfer on the sensor's surface, improving the MIP recognition ability with selectivity and repeatability higher than previously reported sensors and HPLC determinations. The sensor was applied to water, milk, and pork samples as proof of concept. Its recovery ranged from 95 to 106%.

A new strategy consisting of histamine pre-concentration on magnetic MIP@Fe_3O_4 NPs was proposed for histamine allergen determination [20]. The determined LOD was as low as 1.6×10^{-6} mg L^{-1}. Those highly selective NPs allowed extraction of the analyte of different concentrations from the analyte-containing solution or any complex matrix using a constant magnetic field. Therefore, this strategy is useful in separating analytes from a complex food matrix. The histamine recovery in real fish samples ranged between 96.8 and 102.0% with the sensor devised.

3.1.3. Anodic stripping voltammetry (ASV) MIP chemosensors

Somnet et al. devised a sensor constructed of platinum NPs immobilized at an MIP, deposited on graphene coating a screen-printed electrode, (PtNPs@MIP)/graphene/SPE, for a paraquat herbicide determination (Scheme 3a) [23]. The linear dynamic concentration range and LOD of paraquat were 0.05–1000 μM and 0.02 μM, respectively. The sensor was applied to extracts of different vegetables, with the recovery exceeding 93%. Graphene has unique properties, including high chemical stability, conductivity, and biocompatibility, whereas PtNPs@MIP is electrocatalytic. Moreover, the high specific surface area of PtNPs is why the number of active imprinted sites on the surface was high. The synergy effect of these materials significantly increased the electron transfer rate and population of active molecular recognition sites and amplified the sensor's signal, increasing selectivity, repeatability, and stability.

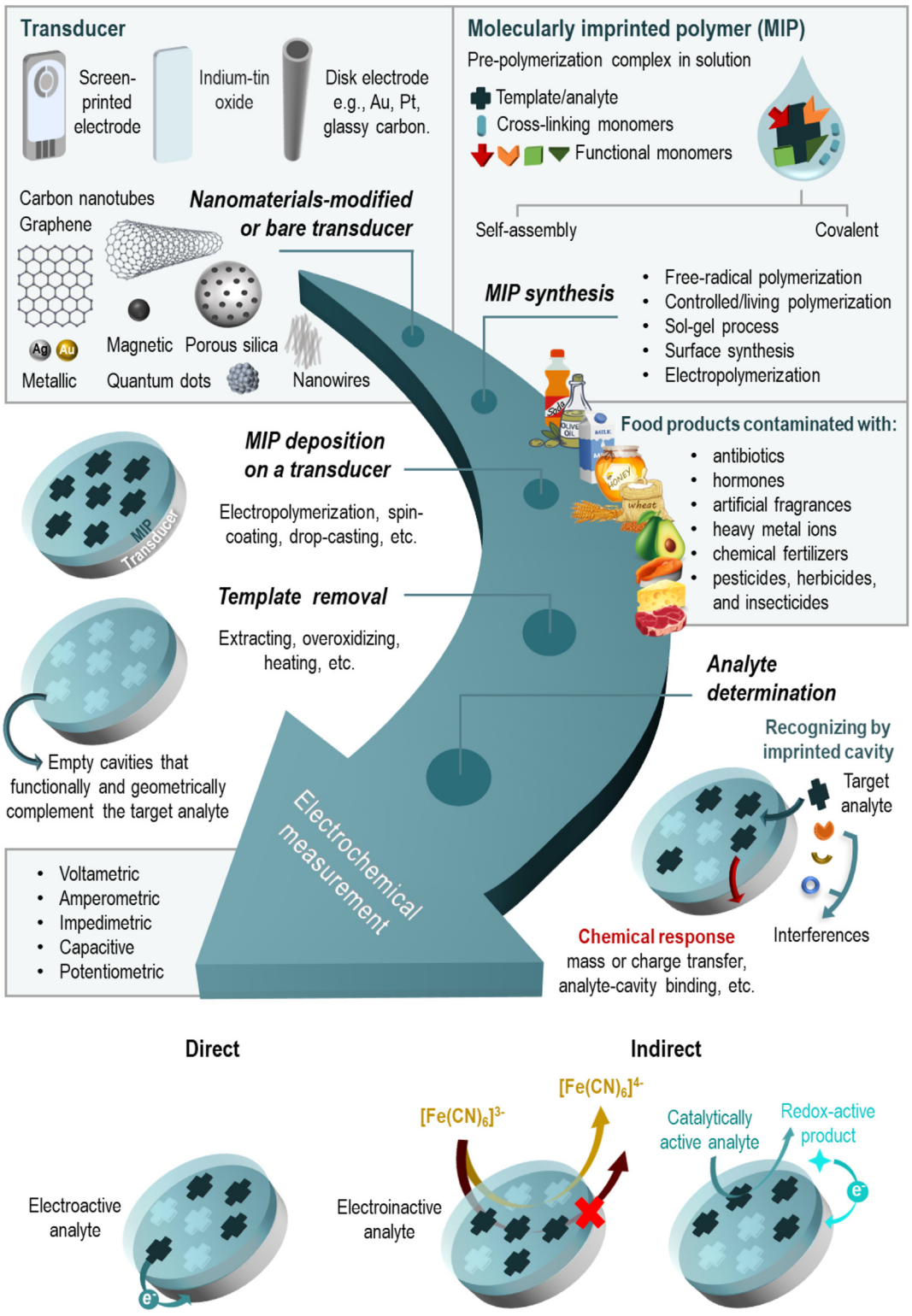

Scheme 1. The basic principle of molecular imprinting, modes of electrochemical measurements, and approaches opted to determine the electroactive, electroinactive, and catalytically active analytes.

3.1.4. Differential pulse voltammetry (DPV) MIP chemosensors

Combining a new material, Au nanostars, deposited on GCE, and parameters' optimization with statistical tools, i.e., central composite design and surface methodology, resulted in a highly selective and sensitive MIP-based chemosensor for a perfluorooctanoic acid potassium salt (PFOS) industrial emulsifier (Scheme 3b) [32]. Ferrocenecarboxylic acid (FcCOOH) was used in this chemosensor system as the redox probe. The chemosensor was superior to other sensors devised for PFOS, where the analytical signal saturated at 1 nM PFOS [46]. This chemosensor overcame the previously reported limitation revealing linearity of 0.05–5.0 nm PFOS with a LOD of 0.015 nm PFOS. Moreover, as proof of concept, the

Table 1
Examples of electrochemical MIP chemosensors' application for contaminants sensing in food samples.

Assay type	Specific target and its group of contaminants	Template, functional, and cross-linking monomer(s)	Sensor fabrication	Assay mode and the probe	Linear dynamic concentration range	Limit of detection (LOD)	Real sample	Ref.
Linear sweep voltammetry (LSV)	Amaranth, an artificial colorant and carcinogen.	Amaranth, pyrrole	MWCNT-modified GCE was coated with MIP.	Direct	0.007−1.0 μM, 0.40 −17 μM	0.4 nM	Soft drinks	[22]
Cyclic voltammetry (CV)	Dibutyl phthalate, a plasticizer.	Dibutyl phthalate, MAA, EDGMA	Carboxylate-SiO_2 was coated with MIP and dropped on AuNPs/MWCNTs/GCE.	Indirect, $[Fe(CN)_6]^{3-}$	$10^{-7} - 10^{-2}$ g L^{-1}[a]	5.09×10^{-9} g L^{-1}	Tap water and Chinese baijiu.	[30]
	17β-Estradiol, a hormone	17β-estradiol, 4-aminothiophenol	Nanowell Au film was formed by dissolving Ag from the Ag/Au alloy. Then, the nanowell film was fixed on the Au electrode through S−S bonding. The modified electrode was coated with MIP.	Indirect, $[Fe(CN)_6]^{3-/4-}$	1.0×10^{12} -1.0×10^{-5} M	1.0×10^{-13} M	Water, milk, and pork	[31]
	Histamine, biogenic amine, food rottenness indicator	Histamine, 2-vinyl pyridine, EDGMA	The C=C bond-activated MIP-modified Fe_3O_4@SiO_2 NPs were coated with MIP. A magnetic field collected the histamine pre-concentrated NPs on a graphite-epoxy composite magneto-actuated electrode.	Direct, pre-concentrated histamine on NPs	0−11.1 mg L^{-1}[b]	1.6×10^{-6} mg L^{-1}	Fish	[20]
Anodic stripping voltammetry (ASV)	Paraquat, a herbicide	Paraquat, MAA, EDGMA	The PtNPs@SiO_2-vinyl NPs were coated with MIP. The NPs were then drop-cast on graphene-modified SCPE.	Direct	0.05−1000 μM	0.02 μM	Vegetables	[23]
Differential pulse voltammetry (DPV)	Perfluorooctane sulfonate, a pollutant	Perfluorooctanoic acid potassium salt, *o*-PD	Au nanostar/GCE was coated with MIP.	Indirect, FcCOOH	0.05−5.0 nm	0.015 nm	Tap water	[32]
	Genistein, a food allergen	Genistein, *o*-PD	SCPE was coated with MIP.	Direct	100 ppb−10 ppm	100 ppb	Soy milk, cookies, muffins, and sauces	[21]
	p-Synephrine, a hazardous dietary supplement	*p*-Synephrine, *bis*-bithiophene derivatized with carboxyl and ferrocene moieties	The Pt electrode was coated with polythiophene-based MIP film.	Indirect, ferrocene moiety co-polymerized in MIP film	0.2−75 nM	0.57 nM	Dietary supplement for body-building	[43]
	Sulfapyridine, a veterinarian drug	Sulfapyridine, MAA, EDGMA	$Ni(OH)_2$ nanoarrays' modified nickel nanofoam electrode was coated with MIP.	Indirect, K_3 $[Fe(CN)_6]$	5.9×10^{-7} − 1.34×10^{-3} M	3.57×10^{-7} M	Fish	[33]
Square wave voltammetry (SWV)	Ochratoxin A, mycotoxin	Ochratoxin A (OTA), ochratoxin D (OTA)	CNT/MoS_2/FMNS, decorated with pIL and AuNPs composite, was coated with MIP.	Indirect, ochratoxin A oxidation product and FMNS serve as the signal and reference probe	0.5−15 mM	14 nM	Chinese liquor, beer, and red wine	[44]
	Citrinin, mycotoxin	Citrinin, thionine	Boron and nitrogen-doped hierarchical porous carbon decorated with pIL on GCE was coated with MIP.	Indirect, $[Fe(CN)_6]^{3-/4-}$ and polythionine serves as signal and reference probe	$1 \times 10^{-3} - 10$ ng mL^{-1}	1×10^{-4} ng mL^{-1}	Red yeast and rice, and wheat	[34]
	Zearalenone, mycotoxin	Coumarin-3-carboxylic acid (dummy), 4-aminothiophenol	pIL functionalized boron-doped ordered mesoporous carbon -AuNPs (BC-AuNPs) coated with zearalenone-templated MIP dropped on GCE.	Indirect, $[Fe(CN)_6]^{3-/4-}$	$5 \times 10^{-4} - 1$ ng mL^{-1}[a]	1×10^{-4} ng mL^{-1}	Corn, rice, and beer	[35]
Amperometry and chrono-amperometry	Gluten, food allergen	Gluten, MAA, EGDMA	MIP was synthesized on Fe_3O_4 NPs' surfaces. Then, the core-shell NPs were spin-coated on SCPE.	Direct	5−50 ppm	1.50 ppm	Crackers	[24]
	Bisphenol A, a pollutant	Bisphenol A, MMA, EGDMA	MIP was synthesized on Fe_3O_4 NPs' surfaces. Then, the core-shell NPs were spin-coated on SCPEs.	Direct	1.0×10^{-8} − 3.0×10^{-6} M	2.053×10^{-8} M	Tap and mineral water and cola	[49]
	Carbofuran, a pesticide	Carbofuran, MAA, trimethylolpropane trimethacrylate	NH_2-functionalized MIP NPs' surface was coupled with the carboxylated-Fe_3O_4@Au core via covalent amide bonds. The NPs were dispersed in a Nafion solution, then dropped onto a GCE.	Direct	0.01−100 μM	1.7 nM	Fruits and vegetable	[50]

(*continued on next page*)

Table 1 (*continued*)

Assay type	Specific target and its group of contaminants	Template, functional, and cross-linking monomer(s)	Sensor fabrication	Assay mode and the probe	Linear dynamic concentration range	Limit of detection (LOD)	Real sample	Ref.
Electrochemical impedance spectroscopy (EIS)	Dichlorodiphenyltrichloroethane, insecticide	Bisphenol A (dummy template), dopamine	Core-shell Fe_3O_4@polydopamine MIP NPs were deposited on the GCE.	Indirect measurement in presence of $[Fe(CN)_6]^{3-/4-}$	1×10^{-11} – 1×10^{-3} M[a]	6×10^{-12} M	Radish	[36]
Capacitive impedimetry (CI)	2-Amino-3,7,8-trimethyl-3*H*-imidazo [4,5-*f*]quinoxaline (7,8-DiMeIQx), carcinogen	7,8-DiMeIQx, thiophene-based monomers bearing adenine and thymine	Nucleobase functionalized polythiophene-MIP thin film was deposited on the Au electrode.	Direct	47–400 μM	15.5 μM	Pork meat	[28]
	Imidacloprid, insecticide	Imidacloprid, MAA, EGDMA	MIP NPs were suspended in tyramine solution, then polymerized on the Au electrode surface.	Direct	5–100 μM	4.61 μM	Tap water	[29]
	E. coli, bacteria	*E. coli* solution, polydimethylsiloxane	*E. coli* solution was spin-coated on a polydimethylsiloxane stamp. The stamp was pressed onto the polyurethane-urea-diamine-coated aluminum chip and then polymerized.	Direct	0–1.0×10^5 CFU/mL[b]	120 CFU/mL	–	[5]
Potentiometry	Pb^{2+}, heavy-metal ion	Pb^{2+}, 2,2′:6′,6″-terpyridine, EGDMA	MIP NPs were dispersed in the PVC, NPOE, NATPB, and THF solution to form an MIP-PVC ionophore membrane. Then, the membrane was dropped on MWCNT/polyaniline-graphite electrode.	Sorption-desorption of ions	5.3×10^{-10} –1.0×10^{-1} M	3.4×10^{-10}	Tap and mineral water	[25]
	Bisphenol AF, a pollutant	Bisphenol AF, divinylbenzene, MAA	MIP was swelled at 150°C for 5 h, then dissolved in the PVC, DOP, TDMAC, and THF solution. Then, the MIP cocktail was drop-cast on GCE.	Sorption-desorption of ions	0.1–1 μM	60 nM	–	
	Dinotefuran, insecticide	Dinotefuran template, acrylamide, EGDMA	The MIP powder was dispersed in a plasticized carboxylated PVC and DOB matrix. The membrane was then punched to a disk shape and pasted to a PVC tip clipped in the electrode glass body.	Sorption-desorption of ions	10^{-7} to 10^{-2} M	0.35 μg L^{-1}	Cucumber	[26]
Dual assays								
Differential pulse voltammetry (DPV)	Tyramine, a biogenic amine, an indicator of food rottenness	Tyramine, *bis*-bithiophene derivatized with carboxyl and crown-ether moieties, 2,3-bithiophene	Polythiophene-based MIP film was deposited on the Pt electrode	Indirect, $[Fe(CN)_6]^{3-/4-}$	290 μM –2.64 mM	159 μM	Mozzarella cheese whey	[37]
Electrochemical impedance spectroscopy (EIS)				Indirect, $[Fe(CN)_6]^{3-/4-}$		168 μM	–	
Differential pulse voltammetry (DPV)	Fumonisin B_1, mycotoxin	Fumonisin B_1, NHS, NIPAM, BIS, TBAM, EGMP, NAPMA, TEMED, APS	Silanized glass beads bearing Fumonisin B1 were polymerized with functional and cross-linking monomers. Then, the beads were covalently attached to a PPy-zinc porphyrin composite film-modified Pt electrode.	Indirect, $[Fe(CN)_6]^{3-/4-}$	1 fM – 10 pM[a]	0.03 fM	–	[38]
Electrochemical impedance spectroscopy (EIS)				Indirectly, the electroactive PPy-ZnP was used as an internal redox marker.		0.7 fM	Maize	

[a] Linear response in a semi-log scale.
[b] Non-linear response.

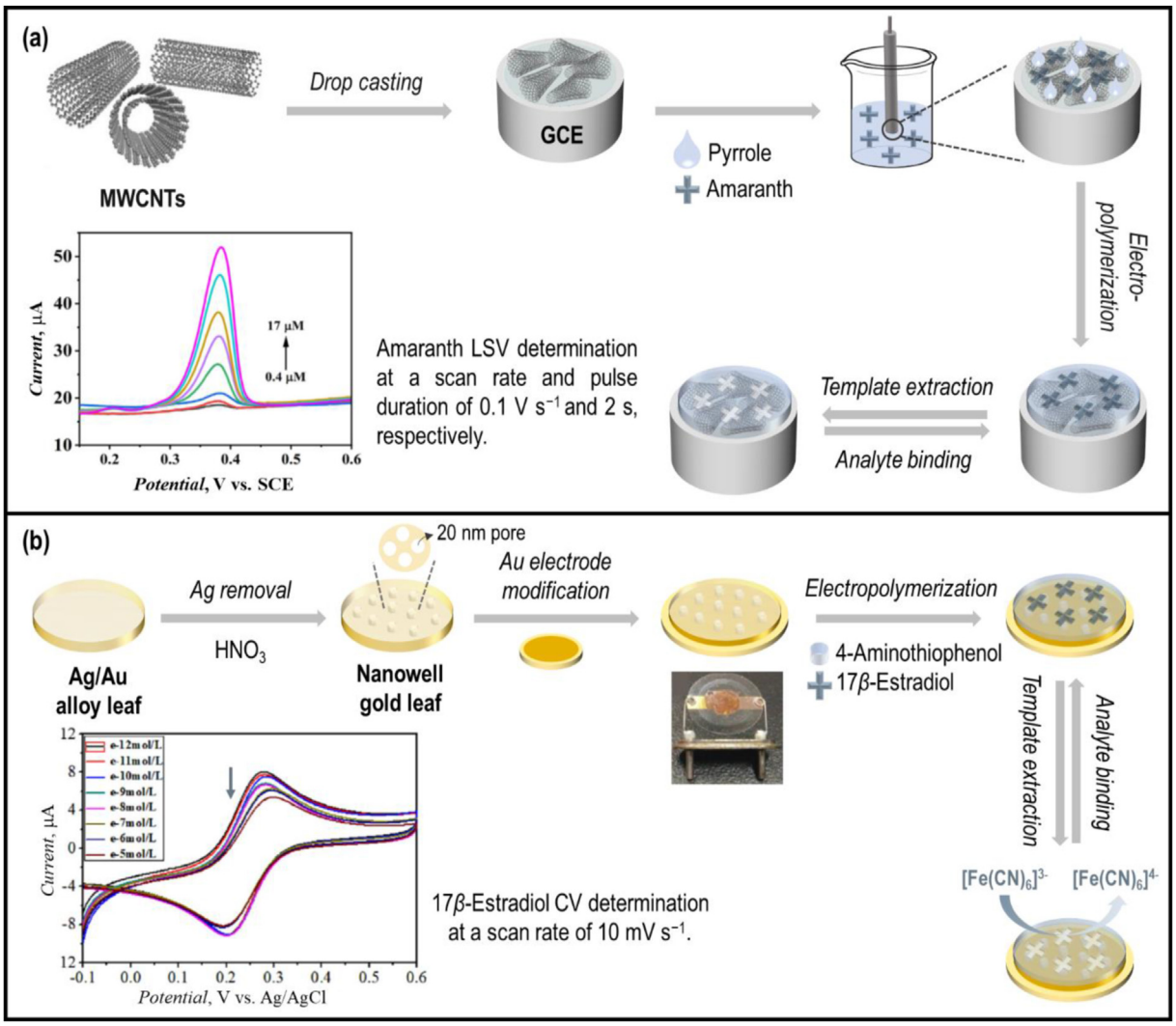

Scheme 2. (a) Amaranth-templated MIP film deposition on the multi-walled carbon nanotubes (MWCNTs) modified glassy carbon electrode (GCE) by electropolymerization. Adapted from Ref. [22]. (b) 17β-Estradiol-templated MIP film deposition on a nanowell gold leaf/gold (Au) electrode by electropolymerization. Adapted from Ref. [31].

chemosensor determined PFOS in tap water, with a recovery of 85.5–89.4%.

Sundhoro et al. proposed a highly selective genistein-templated SPE/MIP as an alternative to commercially available lateral flow devices (LFDs) used for soy allergen determination [21]. The LOD of the SPE/MIP sensor was 100 ppb, exceptional compared to the LOD of the LFDs, i.e., 1–10 ppm. The MIP-based chemosensor selectively determined the allergen in soy milk, sauce, cookies, and muffin samples.

A dual-assay conductive polythiophene film-based MIP chemosensor for tyramine, a catecholamine-releasing agent, clearly demonstrated the superiority of the DPV technique over EIS in terms of quantitative analysis [37]. The calculated apparent imprinting factor (*IF*) and selectivity for DPV assay were higher than for EIS. The *IF* was equal to 5.6 and 2.1, respectively. However, the EIS was very useful in studying the electrode process mechanisms. It was demonstrated that the signal transduction mechanism for the MIP film-coated electrode was different than that at the control electrode coated with a non-imprinted polymer (NIP) film. Only a semicircle and a straight line corresponding to respective R_{ct} and semi-infinitive diffusion were seen for the former. For the control NIP film-coated electrode, EIS spectra were more complex. The NIP film was significantly less conductive and more porous than the MIP film. Therefore, a different equivalent circuit was fitted to EIS spectra for the NIP film-coated electrode. Moreover, analyte binding to the NIP film influenced both overlapped semicircles recorded, one corresponding to the R_{ct} and another originating from a redox probe diffusion through a porous NIP film. Therefore, ΔR_{ct} measuring was complicated. The authors admitted that the *IF* calculated this way was of limited value. Moreover, this result should be considered an important example that calculating *IF* only by comparing MIP and NIP sensors' response is of limited value. Different transduction methods are based on different physicochemical processes. Thus, they can result in different *IF* values for the same MIP/NIP pair. The SPR chips coated with HSA-imprinted polythiophene films were applied in two different assays in another example from the same group [47]. Namely, one was based on surface plasmon resonance (SPR) and another on the birefringence of liquid crystals. The former was sensitive to MIP film electric permittivity changes. The latter responded to changes in MIP film roughness. Therefore, it was more sensitive to interfering proteins' nonspecific adsorption on the film surface. The calculated both *IF* and selectivity were much lower than for the SPR assay. Therefore, we recommend using the term *apparent imprinting factor* if calculated by comparing the MIP and NIP response in a way other than piezomicrogravimetry.

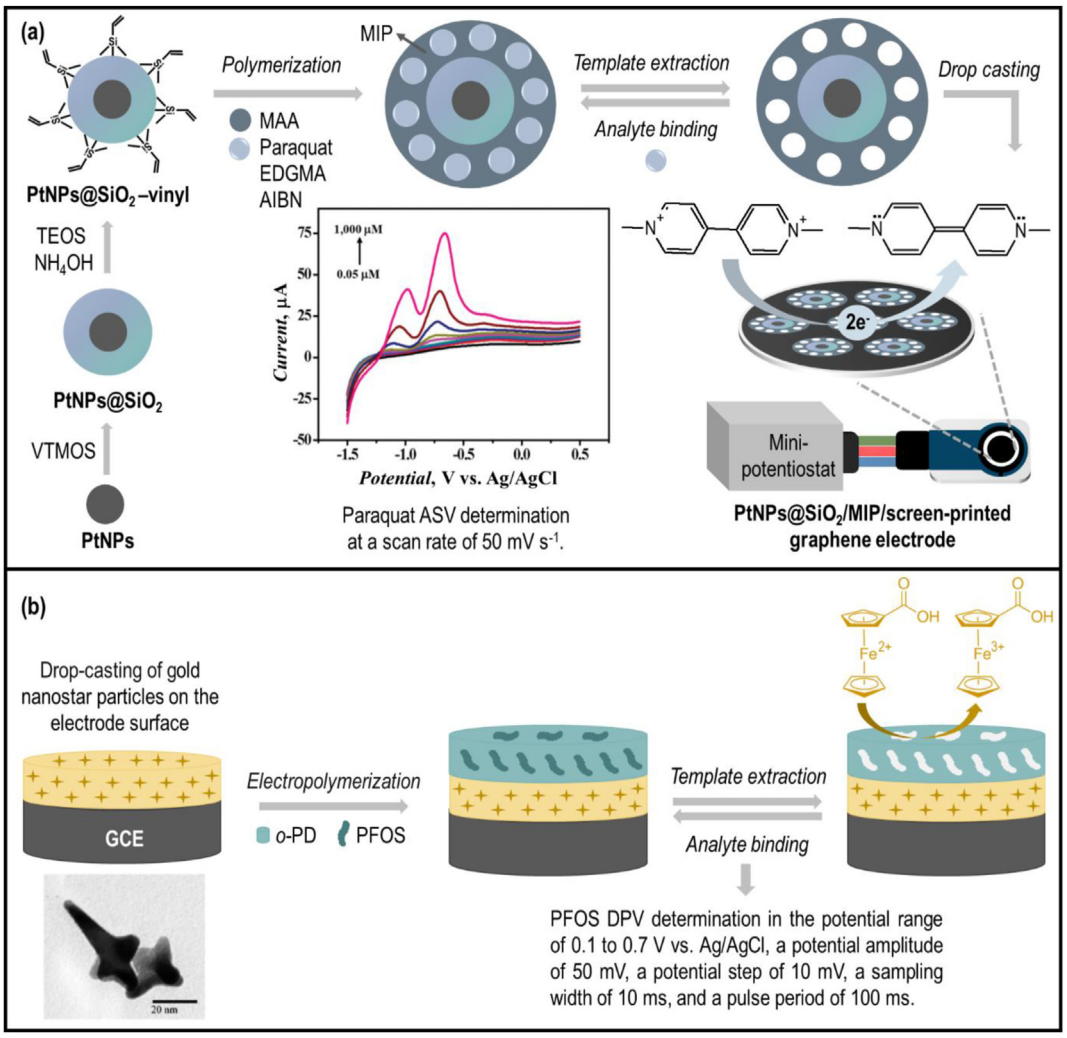

Scheme 3. (a) Paraquat-templated MIP film deposition on the core-shell platinum NPs (PtNPs) and silica dioxide (SiO_2) surface modified with vinyl groups using tetraethoxysilane (TEOS), ammonium hydroxide (NH_4OH), vinyltrimethoxysilane (VTMOS), the methacrylic acid (MAA) functional monomer and the paraquat template. Adapted from Ref. [23]. (b) Electropolymerization of the perfluorooctanoic acid potassium salt (PFOS) template and the *o*-phenylenediamine (*o*-PD) functional monomer on the gold nanostar modified GCE, then analyte DPV determination in the presence of the ferrocenecarboxylic acid (FcCOOH) redox probe. Adapted from Ref. [32].

Liu et al. offered an MIP/$Ni(OH)_2$ nanoarrays/(nickel nanofoam electrode) sensor for antibacterial sulfapyridine medication determination [33]. The $Ni(OH)_2$ surface area, mass transfer rate, operability, and sensitivity are high. Therefore, the MIP chemosensor's reproducibility, stability, and sensitivity were high. The chemosensor was applied to sulfapyridine determination in real freshwater fish samples, with sulfapyridine recovery ranging between 98 and 98.6%.

Moreover, to simplify sample pretreatment and to avoid adding a redox marker to the solution, self-reporting MIP films with ferrocene containing monomer [43], polypyrrole/(zinc porphyrin) composite (PPy-ZnP) [38], or flavin mononucleotide decorated nanotubes [44], build into their structure were deposited on electrodes. This way, the redox process of this immobilized probe was sensitive to the conductivity of the MIP film. Therefore, recorded currents originating from this self-reporting MIP significantly dropped because of analyte binding to the MIP imprinted cavities [43]. These chemosensors were successfully applied for *p*-synephrine [43] and mycotoxins [38,44] determination in dietary supplements [43], alcohol drinks [44], and maize [38].

3.1.5. Square-wave voltammetry (SWV) MIP chemosensors

Hu et al. fabricated an ochratoxin A, OTA, (OTA)-templated MIP using the magnetic field-guided functional monomer alignment simultaneous to promote template complexation on an electrode surface (Scheme 4a). The electrode was firstly decorated with a composite material, namely, (carbon nanotube)/(molybdenum disulfide) (MoS_2)/sodium salt of flavin mononucleotide composite bearing poly(ionic liquid) (pIL) and AuNPs [44]. Then the magnets were placed under the electrochemical cell to orient monomer molecules during electropolymerization, thus resulting in an ordered polymer with uniform imprinting sites. The chemosensor was applied to OTA recovery from the Chinese liquor, beer, and red wine samples. Moreover, the synergy of the nanomaterials' properties contributed to high chemosensor selectivity. The MoS_2 provided a high specific surface area, incurred electrocatalytic activity, and effectively hindered the aggregation of CNTs. CNTs enhanced the electron transfer and, that way, the electrochemical sensor performance. AuNPs amplified the current signal, whereas pIL restricted the aggregation and growth of AuNPs for effective signal amplification.

Boron and nitrogen co-doped hierarchical porous carbon (BN-NPC) was proposed to devise polythionine-based MIP/(BN-NPC)/pIL/GCE for citrinin mycotoxin determination [34]. The electroactive polythionine was utilized because of two purposes. That is, it served as the FM and the internal reference probe for this ratiometric chemosensor. The pIL more orderly anchored the imprinted sites that favored selective citrinin analyte binding to the empty cavities. In combination with high conductivity and large surface area, BN-NPC enhanced the chemosensor's sensitivity and selectivity. As a result, the citrin recovery in a real sample, i.e., red yeast, rice, and wheat, was 97−112%.

pIL-functionalized boron-doped ordered mesoporous carbon-AuNPs, (BC-AuNPs)/GCE was coated with a zearalenone-templated MIP film for zearalenone mycotoxin determination [35]. The multilayer transducer modification increased the chemosensor's conductivity and electrocatalytic activity. The pIL was highly viscous and conductive, and its accessible potential range was wide. Moreover, it assisted the formation of non-aggregated AuNPs on the composite's surface by restricting the NPs' growth, thus enhancing electron transfer. Furthermore, pIL attracted many template molecules to the composite's surface and facilitated their self-assembly with the amino groups on the composite's surface. That increased imprinting sites' density, improving the chemosensor's sensitivity. Moreover, the recovery of zearalenone determination in real corn, rice, and beer samples was high, ranging between 96 and 110%.

3.2. Amperometric and chronoamperometric MIP chemosensors

The amperometric and chronoamperometric chemosensors measure the current change with time, resulting from the electrode process of an electroactive analyte diffusing to the MIP film-coated electrode from the solution bulk. The difference between these two techniques is that the amperometric measurement is performed at a constant voltage or potential, whereas the applied potential is switched in the latter [48]. In both techniques, the current is measured as a function of time obeying the Cottrell equation, which predicts that the current is inversely proportional to the square root of time, $I \propto t^{-1/2}$. Both techniques help measure the current for the diffusion-rate controlled redox process, which linearly increases with the analyte concentration. They are simple yet sensitive, not requiring analyte labeling.

Limthin et al. prepared a highly stable and selective chemosensor of Fe_3O_4@methyl methacrylate deposited on SPE, (Fe_3O_4@MMA)/SPE, to determine possible gluten allergen (Scheme 4b) [24]. MAA is the most reported, commercially available, and inexpensive FM used for MIP-based chemosensor preparation. Unfortunately, MAA is an insulator, hindering charge transfer between an electrode and a test solution, which leads to low sensitivity. To circumvent this drawback, superparamagnetic Fe_3O_4 NPs were introduced to MAA to decrease its electric resistance, thus enhancing the charge transfer. That resulted in a high electric signal and, hence, improved sensitivity. The chemosensor was applied for gluten determination in different flavored crackers. It effectively differentiated gluten-free from gluten-containing crackers.

Moreover, Leepheng et al. determined highly toxic bisphenol A (BPA) using an (Fe_3O_4 NPs@MIP)/SPE sensor [49]. BPA is found in food and beverage plastic packaging. BPA contaminations can cause severe short- and long-term damage to humans. In fact, BPA overdosing can be lethal. The authors reported on a highly selective chemosensor that recognizes BPA in tap, mineral water, and cola samples.

A (Fe_3O_4@Au NPs)/(amino-MIP NPs) chemosensor was fabricated for carbofuran pesticide determination [50]. Toward that, amino groups were introduced on the MIP NPs surface to suitably anchor Fe_3O_4@Au NPs modified with carboxyl groups. This way, (Fe_3O_4@Au NPs)/(amino-MIP NPs) nanocomposite was synthesized. The devised chemosensor sensitivity was high thanks to the large surface-to-volume ratio of the amino-MIP NPs, which offer abundant recognizing sites on the MIP surface. Moreover, the high surface area, high conductivity, and electrocatalytic properties of the Fe_3O_4@Au enhanced the electron transfer between carbofuran molecules and the electrode. As a result, the recovery of the chemosensor applied to carbofuran determination in fruits and vegetables ranged from 98.8 to 104%.

3.3. Impedimetric MIP chemosensors

The impedimetric chemosensor measures the change in film impedance or capacitance upon applying a range of frequencies. Impedimetry is helpful for monitoring changes in film thickness and electric properties, including the change in electric permittivity of the electric double layer originating from analyte-cavity recognition events.

Mioa et al. fabricated Fe_3O_4@polydopamine MIP NPs to determine dichlorodiphenyltrichloroethane (DDT) hazardous insecticides in radish samples (Scheme 5a) [36]. A thoughtful sensor design allowed easy separation of the DDT pre-concentrated by Fe_3O_4@polydopamine MIP NPs from complex samples due to a magnetic field applied. Munawar et al. reported dual-assay, i.e., DPV and EIS, fumonisin B_1 (FB_1) determination with a chemosensor of a Pt electrode coated with a film of a composite of an MIP of polypyrrole-(zinc porphyrin), (MIP NPs)/(Ppy-ZnP)/Pt [38]. The electroactive Ppy-ZnP was used as the redox marker for the EIS measurement. The chemosensor linearly responded to log (FB_1 concentration) in the 1 fM to 10 pM FB_1 range. The LOD for DPV and EIS determinations was 0.03 and 0.7 fM, respectively. The FB_1 impedimetric recovery in maise was 96−102%.

An interesting label-free *E. coli* determination with EIS and the heat-transfer method (HTM), an emerging food analysis method, was proposed using MIP/(diamine functionalized polyurethane-urea)/aluminum chip) [5]. The unique microcontact imprinting procedure resulted in the surface-imprinted film's deposition, with imprints well visible under a scanning electron microscope. The EIS and HTM's respective LODs were 120 and 1070 CFU/mL. The *E. coli* outer cell membrane is charged due to the carboxyl and phosphonate groups presence. Hence, the charge is accumulated at the solid-liquid interface during cavity-(*E. coli*) binding, thus leading to the impedance drop. The charge accumulation influences the impedance relatively more pronouncedly than the thermal resistance, resulting in the overall increased sensitivity of the EIS measurement. Regardless, the HTM was applied to study the chemosensor's selectivity to *S. aureus* and *E. coli* determination in real milk samples. That is because the HTM is superior in cost-effectiveness and does not require complex instrumentation or pretreatment of the real sample. Moreover, the EIS signal noise was higher. Exploring such alternatives to study food matrices is welcome.

3.3.1. Capacitive impedimetry (CI) MIP chemosensors

A polythiophene-based MIP was nucleobase-functionalized to determine, by capacitive impedimetry, 2-amino-3,7,8-trimethyl-3*H*-imidazo [4,5-f]quinoxaline (7,8-DiMeIQx), a potentially cancerogenic heterocyclic aromatic amine (HAA) (Scheme 5b) [28]. The unique design of the chemosensor for 7,8-DiMeIQx utilized the HAAS's ability to intercalate the double-stranded DNA readily. The MIP chemosensor was highly sensitive to the 7,8-DiMeIQx, applied under the steady-state and flow-injection analysis (FIA) conditions. Moreover, the chemosensor was successfully applied to 7,8-DiMeIQx determination in pork meat extract samples.

El-Akaad et al. devised the first [(MIP NPs)-(polytyramine film)]/

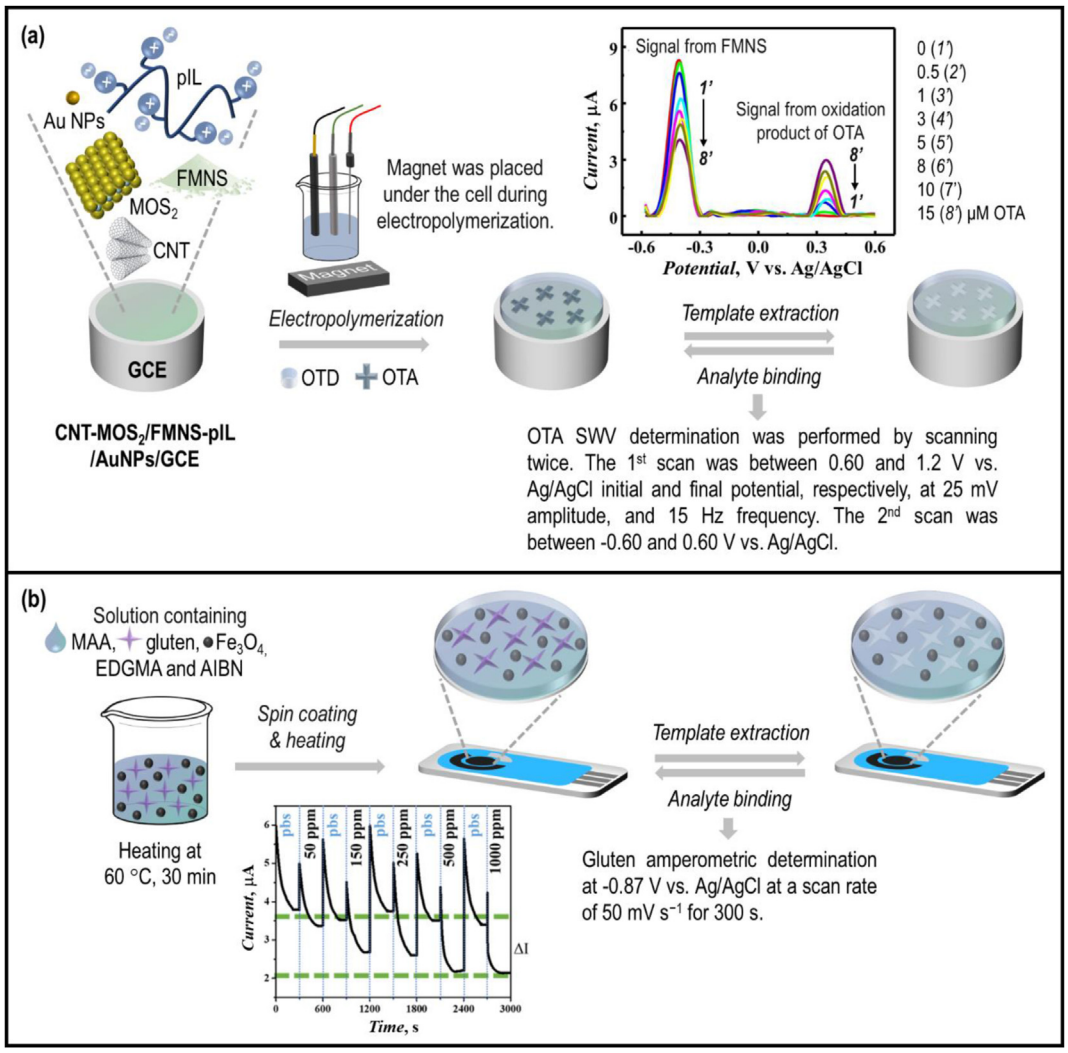

Scheme 4. (a) Electropolymerization, in the presence of a magnetic field, of ochratoxin A (OTA) and ochratoxin D (OTD) on the GCE modified with carbon nanotubes (CNTs), molybdenum disulfide (MoS_2), gold nanoparticles (AuNPs), poly(ionic liquid) (pIL), and sodium salt of flavin mononucleotide (FMNS). Adapted from Ref. [44]. (b) MIP film synthesis on an SPE for amperometric gluten determination. Adapted from Ref. [24].

(Au electrode)capacitive chemosensor to determine an imidacloprid insecticide in water samples, i.e., tap and river water [29]. A two-step chemosensor fabrication procedure involved synthesizing MIP beads by emulsion polymerization and then immobilizing them, suspended in tyramine solution, on the Au electrode surface by electropolymerization. These extensive fabrication steps were afforded to ensure no residual template molecules adhered to the electrode and avoid potential electrode damage. Moreover, before each determination, the modified electrode was allowed to regenerate, which enabled reusing the same electrode as many as 32 times.

3.4. Potentiometric MIP chemosensors

Potentiometric MIP chemosensors measure the potential difference between the indicator and reference electrode, prevailingly under zero-current conditions. The charge accumulated in the MIP film generates the potential difference. This difference can be generated without needing the target analyte to diffuse through the MIP film [45]. Generally, the reference electrode potential is constant, and the indicator electrode potential varies depending on the examined solution composition. The potential difference correlates with the ion activity in solution, equivalent to the concentration, but only at very low concentrations. The potentiometric chemosensor's response is linear against the logarithm of the analyte ion concentration, covering a broad concentration range, as estimated by the Nikolsky-Eisenman equation. Potentiometric chemosensors' advantages include their high selectivity, relatively short response time, easy use, and inexpensive preparation. The downside is their insensitivity to small changes in analyte concentrations because they linearly respond to the logarithm of analyte concentration.

Ardalani et al. developed a simple and inexpensive method to determine lead ion (Pb^{2+}) in the tap and mineral water samples using [MIP-(PVC membrane)]/MWCNTs/polyaniline/(graphite electrode) (Scheme 6) [25]. Polyaniline is a highly conductive polymer that can enhance the signal and improve the sensor's sensitivity. The synergy effect of MWCNTs and polyaniline allowed the chemosensor to reach a LOD down to sub-nano Pb^{2+} concentration, i.e., 3.4×10^{-10} M.

Abdel-Ghany et al. devised a highly selective potentiometric chemosensor for determining a dinotefuran insecticide [26]. Two different MIPs were prepared using acrylamide (AM) or MAA FMs. Apparently, for the template-extracted MIP-AM chemosensor, the

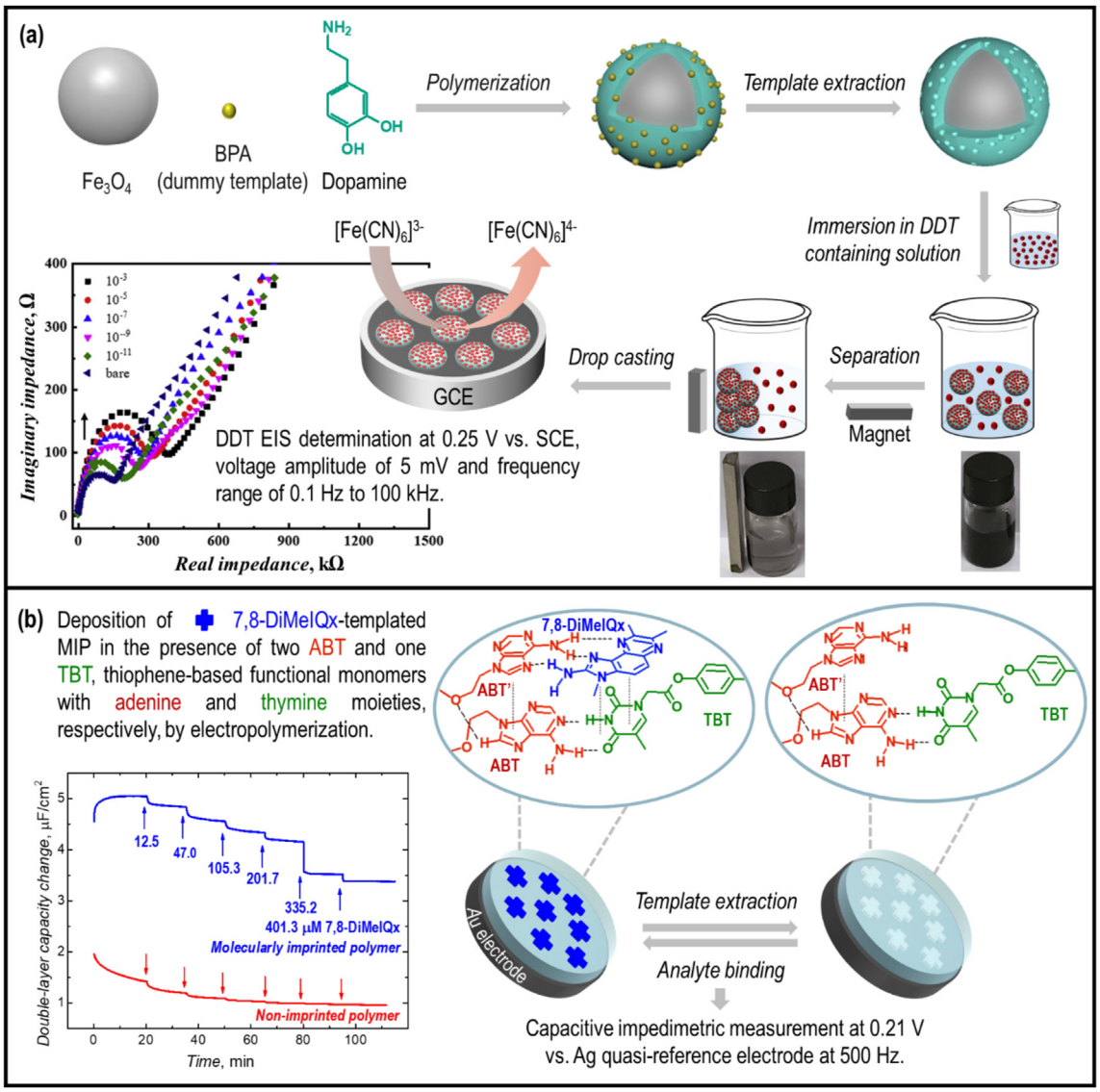

Scheme 5. (a) Core-shell Fe_3O_4@polydopamine MIP NPs/GCE fabrication for dichlorodiphenyltrichloroethane (DDT) EIS determination. Adapted from Ref. [36]. (b) MIP film deposition on an Au electrode by electropolymerization using 4-*bis*(2,2′-bithien-5-yl)methylphenyl 2-adenine ethyl ether (ABT), 4-*bis*(2,2′-bithien-5-yl)methylphenyl thymine-1-acetate (TBT) functional monomers, 2,4,5,2′,4′,5′-hexa(thiophene-2-yl)-3,3′-bithiophene (T8) cross-linking monomer in the presence of 2-amino-3,7,8-trimethyl-3*H*-imidazo [4,5-f] quinoxaline (7,8-DiMeIQx) template. Adapted from Ref. [28].

potentiometric response, *IF*, binding capacity, and sensitivity were the highest, and the LOD was the lowest. This chemosensor was applied to the cucumber samples spiked with dinotefuran; the dinotefuran recovery ranged from 87 to 106%.

One of the common challenges in constructing an MIP-based potentiometric sensor is the insolubility of the MIP receptor in polymer matrices. Often, the MIP particles are heterogeneously dispersed in a plasticized polymer matrix of the membrane [25,26]. That translates into fewer recognizing sites available for molecular recognition. Zhang et al. overcome this drawback by swelling the template-extracted MIP at 150 °C before membrane preparation [27]. Bisphenol AF (BPAF), a more harmful and dangerous analog of BPA, was determined using the chemosensor devised. As expected, this chemosensor's response was superior to the traditionally prepared MIP membrane. Then, river samples were examined. This chemosensor is exceptionally suitable for determining BPA in drinking water and food samples.

4. Future perspectives and unsolved challenges

The MIP sensors field has rapidly grown for the last ten years. Recently, many review articles describing the application of MIP sensors in several fields, namely, clinical diagnosis [51], cancer biomarkers detection [52,53], forensic sciences [54], warfare-agents detection [55], and environmental analysis [51,56,57], were published. This rapid growth highlights the possibility of introducing MIP chemosensors to the market and applying them in everyday practice, i.e., food quality and safety control. However, several issues must be solved before introducing mass production of MIP electrochemical sensors.

It is necessary to control precisely the amount of MIP deposited on the electrode surface to ensure high reproducibility of the MIP

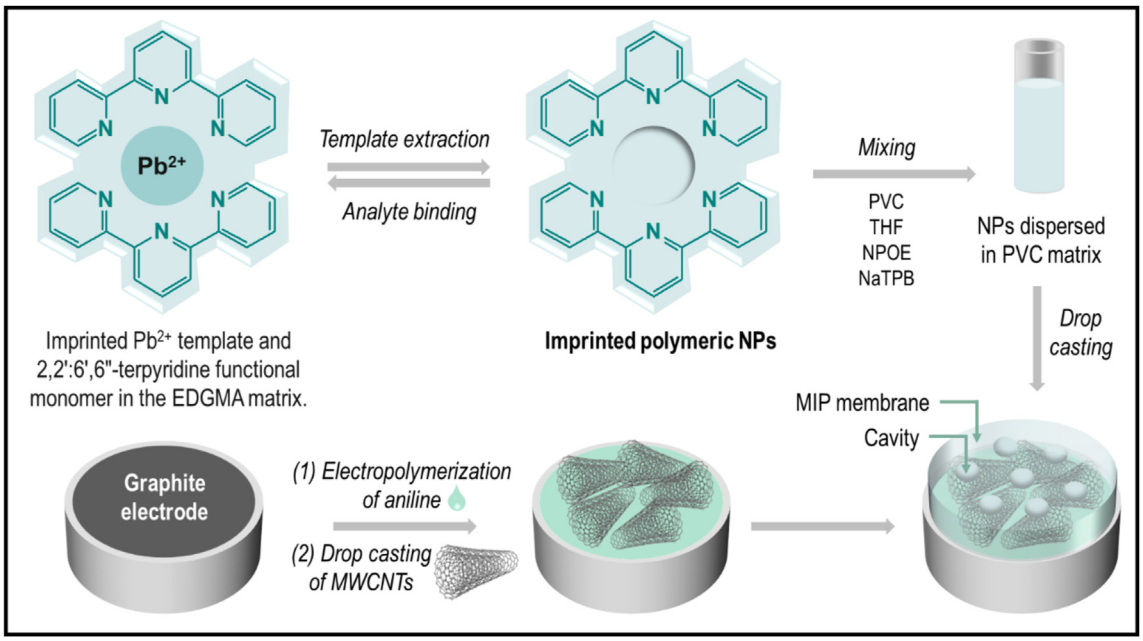

Scheme 6. MIP-poly(vinyl chloride) (PVC) ionophore membrane prepared by dissolving the lead ion (Pb^{2+})-extracted MIP NPs in PVC, 2-nitrophenyl octyl ether (NPOE), sodium tetraphenyl borate (NATPB) in tetrahydrofuran (THF) solvent. Adapted from Ref. [25].

electrochemical sensors. Free-radical polymerization, considered the most common polymerization method, offers scarce control over synthesized MIP amount and morphology. Therefore, electropolymerization seems to be the method of choice for MIP films' deposition on electrode surfaces [58,59]. This method limits the polymerization space only to the electrode surface. The amount of charge passed through the electrode can precisely control the resulting MIP film thickness. Moreover, such features of an MIP film as morphology, i.e., porosity or conductivity, can be tuned by selecting proper electropolymerization conditions. Importantly, suppose the synthesized polymer is non-conductive, i.e., polyphenol or polydopamine. In that case, electropolymerization is a self-limiting process, and the thickness of the deposited MIP film can be controlled with precision equal to several nanometers [59,60]. So-called "living polymerization" is another approach to graft MIP film on the electrode surface with precise control over film thickness [59–61]. In this case, the polymerization is slowed to such an extent that it is possible to stop it after reaching the pending MIP film thickness [62]. However, both approaches work perfectly in laboratories. It is impossible to transfer them to mass-produced inexpensive and easy-to-use sensors. Both polymerization methods require using expensive, toxic, and burdening environment chemicals, including organic solvents, supporting electrolytes, copper catalysts, or/and iniferters. Moreover, each produced electrode must be modified separately. That may be considered as a real challenge for production on an industrial scale.

Up to now, automated systems for MIP NPs synthesis have been reported [63–65], allowing for high-throughput production. Recently, several protocols of electrode printing with conductive inks were proposed [66,67]. Combining these two approaches, i.e., suspending MIP NPs into conductive inks, would enable easy and inexpensive production of single-use selective electrodes by simple printing on a paper support. Moreover, the versatility of the molecular imprinting approach allows tailoring design MIP NPs selective to the numerous chosen analytes. Therefore, such electrodes would be useful in infield analyte determinations for numerous purposes, including food quality control. However, such an attempt has not yet been reported.

5. Conclusions

Devising MIP electrochemical chemosensors for food safety and quality monitoring is an important research topic. Recent developments and innovations in various scientific fields, including materials science and nanotechnology, resulted in significant improvements in electrochemical chemosensors. That has consequently led to the development of many highly selective and sensitive MIP electrochemical sensors, discussed in the present review article. The fast-growing number of reported MIP chemosensors for food contaminants determination indicates that this field is ready for commercialization, and soon we may expect the introduction of these sensors into the market. It would enable fast and easy in-field control of food products quality.

Declaration of competing interest

The authors declare the following financial interests/personal relationships which may be considered as potential competing interests. Maciej Cieplak reports financial support provided by The National Science Centere of Poland. Viknasvarri Ayerdurai reports financial support was provided by EU Framework Programme for Research and Innovation Marie Sklodowska-Curie Actions. Viknasvarri Ayerdurai reports financial support provided by Polish Ministry of Science and Higher Education.

Data availability

No data was used for the research described in the article.

Acknowledgments

The present research was partially funded from the financial resources for science in 2017–2021, awarded by the Polish Ministry of Science and Higher Education for implementing an international co-financed project. Furthermore, the present publication is part of a project that has received funding from the European Union's Horizon 2020 research and innovation program under the Marie

Sklodowska-Curie grant agreement No. 711859. Moreover, the authors acknowledge The National Science Center of Poland for financial support to M.C. (Grant SONATA no. 2018/31/D/ST5/02890).

References

[1] Population, Food Security, Nutrition and Sustainable Development, Department of Economic and Social Affairs, The United Nations, 2021.
[2] Y. Cao, T. Feng, J. Xu, C. Xue, Biosens. Bioelectron. 141 (2019), 111447.
[3] E. Hong, S.Y. Lee, J.Y. Jeong, J.M. Park, B.H. Kim, K. Kwon, H.S. Chun, J. Sci. Food Agric. 97 (2017) 3877.
[4] G. Maduraiveeran, M. Sasidharan, V. Ganesan, Biosens. Bioelectron. 103 (2018) 113.
[5] R. Arreguin-Campos, K. Eersels, J.W. Lowdon, R. Rogosic, B. Heidt, M. Caldara, K.L. Jiménez-Monroy, H. Diliën, T.J. Cleij, B. van Grinsven, Microchem. J. 169 (2021), 106554.
[6] J.J. BelBruno, Chem. Rev. 119 (2019) 94.
[7] P. Regal, M. Díaz-Bao, R. Barreiro, A. Cepeda, C. Fente, Open Chem 10 (2012) 766.
[8] A.N. Kozitsina, T.S. Svalova, N.N. Malysheva, A.V. Okhokhonin, M.B. Vidrevich, K.Z. Brainina, Biosensors 8 (2018) 35.
[9] A. Vasilescu, G. Nunes, A. Hayat, U. Latif, J.L. Marty, Sensors 16 (2016) 1863.
[10] P.S. Sharma, M. Dabrowski, F. D'Souza, W. Kutner, TrAC, Trends Anal. Chem. 51 (2013) 146.
[11] H. Lu, H. Tian, C. Wang, S. Xu, Mater. Adv. 1 (2020) 2182.
[12] G. Ozcelikay, S.I. Kaya, E. Ozkan, A. Cetinkaya, E. Nemutlu, S. Kır, S.A. Ozkan, TrAC, Trends Anal. Chem. 146 (2022), 116487.
[13] N. Leibl, K. Haupt, C. Gonzato, L. Duma, Chemosensors 9 (2021) 123.
[14] M.I. Malik, H. Shaikh, G. Mustafa, M.I. Bhanger, Separ. Purif. Rev. 48 (2019) 179.
[15] K.A. Sarpong, W. Xu, W. Huang, W. Yang, Am. J. Anal. Chem. 10 (2019) 202.
[16] C.I.L. Justino, A.C. Freitas, R. Pereira, A.C. Duarte, T.A.P. Rocha Santos, TrAC, Trends Anal. Chem. 68 (2015) 2.
[17] J. Riu, B. Giussani, TrAC, Trends Anal. Chem. 126 (2020), 115863.
[18] S. Kurbanoglu, C. Erkmen, B. Uslu, TrAC, Trends Anal. Chem. 124 (2020), 115809.
[19] B. Cui, P. Liu, X. Liu, S. Liu, Z. Zhang, J. Mater. Res. Technol. 9 (2020), 12568.
[20] A.H.A. Hassan, L. Sappia, S.L. Moura, F.H.M. Ali, W.A. Moselhy, M. Sotomayor, M.I. Pividori, Talanta 194 (2019) 997.
[21] M. Sundhoro, S.R. Agnihotra, B. Amberger, K. Augustus, N.D. Khan, A. Barnes, J. BelBruno, L. Mendecki, Food Chem. 344 (2021), 128648.
[22] Y. Wu, G. Li, Y. Tian, J. Feng, J. Xiao, J. Liu, X. Liu, Q. He, J. Electroanal. Chem. 895 (2021), 115494.
[23] K. Somnet, S. Thimoonnee, C. Karuwan, W. Kamsong, A. Tuantranont, M. Amatatongchai, Analyst 146 (2021) 6270.
[24] D. Limthin, P. Leepheng, A. Klamchuen, D. Phromyothin, Polymers 14 (2022) 91.
[25] M. Ardalani, M. Shamsipur, A. Besharati-Seidani, J. Electroanal. Chem. 879 (2020), 114788.
[26] M.F. Abdel-Ghany, L.A. Hussein, N.F. El Azab, Talanta 164 (2017) 518.
[27] H. Zhang, R.Q. Yao, N. Wang, R.N. Liang, W. Qin, Anal. Chem. 90 (2018) 657.
[28] V. Ayerdurai, A. Garcia-Cruz, J. Piechowska, M. Cieplak, P. Borowicz, K.R. Noworyta, G. Spolnik, W. Danikiewicz, W. Lisowski, A. Pietrzyk-Le, F. D'Souza, W. Kutner, P.S. Sharma, J. Agric. Food Chem. 69 (2021), 14689.
[29] S. El-Akaad, M.A. Mohamed, N.S. Abdelwahab, E.A. Abdelaleem, S. De Saeger, N. Beloglazova, Sci. Rep. 10 (2020), 14479.
[30] S. Wang, M. Pan, K. Liu, X. Xie, J. Yang, L. Hong, S. Wang, Food Chem. 381 (2022), 132225.
[31] T. Wen, M. Wang, M. Luo, N. Yu, H. Xiong, H. Peng, Food Chem. 297 (2019), 124968.
[32] D. Lu, D.Z. Zhu, H. Gan, Z. Yao, J. Luo, S. Yu, P. Kurup, Sens. Actuators, B 352 (2022), 131055.
[33] Z. Liu, Y. Zhang, J. Feng, Q. Han, Q. Wei, Sens. Actuators, B 287 (2019) 551.
[34] X. Hu, Y. Liu, Y. Xia, F. Zhao, B. Zeng, Food Chem. 363 (2021), 130385.
[35] X. Hu, C. Wang, M. Zhang, F. Zhao, B. Zeng, Talanta 217 (2020), 121032.
[36] J. Miao, A. Liu, L. Wu, M. Yu, W. Wei, S. Liu, Anal. Chim. Acta 1095 (2020) 82.
[37] V. Ayerdurai, M. Cieplak, K.R. Noworyta, M. Gajda, A. Ziminska, M. Sosnowska, J. Piechowska, P. Borowicz, W. Lisowski, S. Shao, F. D'Souza, W. Kutner, Bioelectrochemistry 138 (2021), 107695.
[38] H. Munawar, A. Garcia-Cruz, M. Majewska, K. Karim, W. Kutner, S.A. Piletsky, Sens. Actuators, B 321 (2020), 128552.
[39] Y. Yoshimi, R. Ohdaira, C. Iiyama, K. Sakai, Sens. Actuators, B 73 (2001) 49.
[40] Y. Yoshimi, A. Narimatsu, K. Nakayama, S. Sekine, K. Hattori, K. Sakai, J. Artif. Organs 12 (2009) 264.
[41] P. Lach, M. Cieplak, M. Majewska, K.R. Noworyta, P.S. Sharma, W. Kutner, Anal. Chem. 91 (2019) 7546.
[42] R.K. Franklin, S.M. Martin, T.D. Strong, R.B. Brown, Chemical and Biological Systems: Chemical Sensing Systems for Liquids, Elsevier, 2016.
[43] P. Lach, M. Cieplak, K.R. Noworyta, P. Pieta, W. Lisowski, J. Kalecki, R. Chitta, F. D'Souza, W. Kutner, P.S. Sharma, Sens. Actuators, B 344 (2021), 130276.
[44] X. Hu, Y. Xia, Y. Liu, Y. Chen, B. Zeng, Sens. Actuators, B 359 (2022), 131582.
[45] M.C. Blanco-López, M.J. Lobo-Castañón, A.J. Miranda-Ordieres, P. Tuñón-Blanco, TrAC, Trends Anal. Chem. 23 (2004) 36.
[46] R. Kazemi, E.I. Potts, J.E. Dick, Anal. Chem. 92 (2020), 10597.
[47] M. Cieplak, R. Weglowski, Z. Iskierko, D. Weglowska, P.S. Sharma, K.R. Noworyta, F. D'Souza, W. Kutner, Sensors 20 (2020) 4692.
[48] V. Gaudin, in: A.A. Ensafi (Editor), Chapter 11 - Receptor-Based Electrochemical Biosensors for the Detection of Contaminants in Food Products, Elsevier, 2019, p. 307.
[49] P. Leepheng, D. Limthin, K. Onlaor, B. Tunhoo, D. Phromyothin, T. Thiwawong, Jpn. J. Appl. Phys. 60 (2021) SCCJ03.
[50] M. Amatatongchai, S. Thimoonnee, P. Jarujamrus, D. Nacapricha, P.A. Lieberzeit, Microchem. J. 158 (2020), 105298.
[51] Y.L. Mustafa, A. Keirouz, H.S. Leese, J. Mater. Chem. B 10 (2022) 7418.
[52] G. Selvolini, G. Marrazza, Sensors 17 (2017) 718.
[53] S. Bhakta, P. Mishra, Sens. Actuator. Rep. 3 (2021), 100061.
[54] E. Yılmaz, B. Garipcan, H. Patra, L. Uzun, Sensors 17 (2017) 691.
[55] M. Grabka, Z. Witkiewicz, K. Jasek, K. Piwowarski, Sensors 22 (2022) 5607.
[56] P. Rebelo, E. Costa-Rama, I. Seguro, J.G. Pacheco, H.P.A. Nouws, M.N.D.S. Cordeiro, C. Delerue-Matos, Biosens. Bioelectron. 172 (2021), 112719.
[57] B. Keitel, A.D. Batista, B. Mizaikoff, B. Fresco-Cala, Molecularly Imprinted Polymer Sensors for Environmental Analysis. Encyclopedia of Sensors and Biosensors 4, Elsevier B.V., 2022, pp. 851–867.
[58] P.S. Sharma, A. Pietrzyk-Le, F. D'Souza, W. Kutner, Anal. Bioanal. Chem. 402 (2012) 3177.
[59] J. Erdőssy, V. Horváth, A. Yarman, F.W. Scheller, R.E. Gyurcsányi, TrAC, Trends Anal. Chem. 79 (2016) 179.
[60] M. Dabrowski, P. Lach, M. Cieplak, W. Kutner, Biosens. Bioelectron. 102 (2018) 17.
[61] I. Veloz Martínez, J.I. Ek, E.C. Ahn, A.O. Sustaita, RSC Adv. 12 (2022) 9186.
[62] Y. Kamon, R. Matsuura, Y. Kitayama, T. Ooya, T. Takeuchi, Polym. Chem. 5 (2014) 4764.
[63] F. Canfarotta, A. Poma, A. Guerreiro, S. Piletsky, Nat. Protoc. 11 (2016) 443.
[64] S. Ambrosini, S. Beyazit, K. Haupt, B.T.S. Bui, Chem. Commun. 49 (2013) 6746.
[65] J.J. Xu, S. Ambrosini, E. Tamahkar, C. Rossi, K. Haupt, B.T.S. Bui, Biomacromolecules 17 (2016) 345.
[66] S. Mekhmouken, N. Battaglini, G. Mattana, A. Maurin, S. Zrig, B. Piro, D. Capitao, V. Noel, Electrochem. Commun. 123 (2021), 106918.
[67] D. Soulis, M. Trachioti, C. Kokkinos, A. Economou, M. Prodromidis, Sensors 21 (2021) 6908.